

DESIGN OF A TAGGED PHOTON-ELECTRON BEAM FACILITY FOR NAL

C. Halliwell, P. J. Biggs, W. Busza, M. Chen, T. Nash
F. Murphy, G. Luxton, and J. D. Prentice

March 1972



DESIGN OF A TAGGED PHOTON-ELECTRON BEAM FACILITY FOR NAL

C. Halliwell
Carleton University
Ottawa, Canada

and

P. J. Biggs, W. Busza, M. Chen, and T. Nash
Massachusetts Institute of Technology
Cambridge, Massachusetts

and

F. Murphy
University of California
Santa Barbara, California

and

G. Luxton
University of California
Santa Cruz, California

and

J. D. Prentice
University of Toronto
Toronto, Canada

ABSTRACT

We present a design for a tagged photon-electron facility for the National Accelerator Laboratory. This facility is designed to provide tagged photons with energy from 15-300 GeV and electrons up to 300 GeV with energy resolution of $\pm \sim 2.0\%$. For 10^{13} incident 500-GeV protons we expect typically 1.5×10^8 electrons at 150 GeV and 5×10^5 photons with $100 \text{ GeV} < E < 150 \text{ GeV}$. Photons from π^0 's produced in

a primary target by proton interactions are separated from charged secondaries and then allowed to convert to e^+e^- in a Pb radiator. The electrons are transported either to an experimental target or to a second radiator where they may produce photons with tagged energy. Hadronic contamination is kept below a few tenths of a percent.

I. INTRODUCTION

We report here the design of an electron/tagged photon beam for energies up to 300 GeV at the National Accelerator Laboratory. This design results from the collaborative efforts of physicists representing all three presently proposed experiments that require a tagged photon beam.

The basic principles of this design¹ are shown schematically in Fig. 1. A high-energy extracted proton beam incident on a low Z target such as Be produces π^0 's which decay to photons. The photons go forward for about 22 m to a Pb radiator where they convert to e^+e^- . Protons that passed through the primary target as well as charged secondary particles are swept away from the radiator by a series of bending magnets. After the radiator a negatively charged beam is selected, momentum analyzed, and focused 307.5 m downstream. At a distance of about 40 m before the final focus the electrons may be converted to photons in a second Pb radiator. The recoiling electrons are detected and momentum analyzed in order to tag the energy of the photons which then proceed essentially in the same direction as the beam electrons to the final focus at the experimental target.

With a 500-GeV beam of 10^{13} protons/pulse, one can expect a bremsstrahlung distribution of 5×10^5 tagged photons/pulse in the range $100 \text{ GeV} < E < 150 \text{ GeV}$. If the second radiator is removed there will be $\sim 1.5 \times 10^8 e^-$ /pulse incident on the experimental target at 150 GeV.

The model assumptions that go into these estimates and estimates at other energies will be discussed in Section V. Whether in use as an electron or photon beam, the initial version of this facility will have an energy resolution of $\pm \sim 2\%$ (fwhm).

The design of this beam is strongly influenced by considerations aimed at keeping background fluxes at acceptably low levels. We shall discuss later the details of the mechanisms involved and the means of reducing them. Here we simply note the three types of background that warrant consideration:

(1) Neutrons produced in the primary target will not be swept away before hitting the Pb radiator. In the radiator they will produce, among other things, π^- which are transported along with the electrons. In the tagging radiator, the π^- produce neutrons which can interact strongly in the experimental target. A factor of at least 100 discrimination against pions in the tagging system makes this problem less serious when the facility is used for photons than for electrons. A π/e ratio of 10^{-3} to 10^{-4} can be obtained with this beam by appropriate collimation and by steering the incident protons at small angles from 0° .

(2) Muons coming from the primary target (and the beam dump) have sufficient energy to go through many hundreds of feet of earth. This requires the beam to be at least 300 m long and bent ~ 8 m from the incident proton direction at the experimental area.

(3) Electrons that scrape the edge of a magnet or a beam pipe can

in principle cause showers of low-energy particles that might cascade downstream as a low-energy halo. We have found that this kind of a halo can be kept at an acceptably low level by taking the precautions of keeping losses to nearly zero in the last half of the beam, by including sweeping magnets as the last beam elements before the tagging system, and by specifying a beam-pipe diameter larger than 20 cm.

II. THE FRONT END

Immediately before the primary target a series of bending magnets provide the flexibility of steering the proton beam onto the target at angles up to a few milliradians relative to the 0° line of the subsequent beam. As will be discussed in Section VI, a 2-mrad proton angle reduces the π/e background ratio by a factor of ~ 5 while only reducing the electron yield by 2 to 3. A flexible steering angle is thus required in case measured π/e ratios turn out to be higher than predicted. If μ fluxes become a problem, the flexible proton incident angle would again be useful.

The choice of material for the primary target is determined by requiring maximum π^0 production and minimum electromagnetic attenuation of the decay photons. In other words, we require a minimum collision-to-radiation length ratio. This ratio, α , is smallest for low Z elements. Be has the lowest ratio among stable metals and is therefore a good choice for target.

We have integrated the attenuation of the incident proton and the secondary photons and neutrons over the length of the target. We find

that the yield of electrons or photons and the n/γ or π/e ratio depends as follows² on the target length, T , in units of collision length:

$$e \propto \frac{e^{-T} - e^{-0.77\alpha T}}{0.77\alpha - 1} Y_{\pi^0}(A, Z); \quad \frac{\pi}{e} \propto \frac{(0.77\alpha - 1)Te^{-T}}{e^{-T} - e^{-0.77\alpha T}} \frac{Y_n(A, Z)}{Y_{\pi}(A, Z)}$$

Here $Y_{\pi^0}(A, Z)$ and $Y_n(A, Z)$ are the yields per interacting proton and are independent of target thickness. The π/e ratio improves steadily with increasing thickness. On the other hand, the photon-electron yield reaches a peak and then decreases with increasing thickness as more and more photons are attenuated. The peak represents the ideal operating thickness and may be located empirically. For Be we use³ $\alpha = 0.86$, for which the operating thickness is about 1.2 coll. lengths or 36 cm.

Another possible choice for target is D_2 with³ $\alpha = 0.29$. For D_2 the peak comes at 1.9 coll. lengths (~400 cm). The yields will increase by 60% because of the longer lengths (in units of c.l.). Theoretically, an even greater increase is expected because of lower nuclear absorptions. The π/e background ratio improves by a factor of 2. On the other hand, there are serious engineering difficulties in maintaining a 4-m long liquid D_2 target in which 10^{13} 500-GeV protons/pulse are losing more than 500 W.

Immediately following the target, a series of sweeping magnets bend the charged particles down to a beam dump. In order to miss the edge of the first quadrupole 29 m downstream, the minimum deflection must be 16 cm. A bending power of 170 kg-m over the first 9 m will be sufficient to deflect 500 GeV/c particles 25 cm at the quadrupole.

The radiator is located about 22 m away from the target. The transverse size of the radiator is about $1 \text{ cm} \times 1 \text{ cm}$ (determined by the angular acceptance of the beam transport) so that the deflected protons will easily pass by. Lead is chosen for the radiator since we require a very high collision length-to-radiation length ratio to maximize radiative effects (pair production) and minimize strong interactions (pion production). A Monte Carlo program which was used to estimate yields (Section V) indicates that the optimum operating thickness for the Pb radiator will be about 0.5 r.l. or 2.9 mm. The calculation takes into account the attenuation of the e^- , the pair-production dynamics, e^- straggling, as well as neutron and pion attenuation. As shown in Fig. 2, the calculation predicts that e^- yields will rise to a plateau starting at ~ 0.5 r.l., while the π/e ratio increases steadily. In practice the Pb thickness will be optimized empirically.

III. THE ELECTRON TRANSPORT

The beam-transport system has been designed to fulfill the following requirements which are considered necessary for all three proposed tagged-photon experiments:

- (1) The final focus is located ~ 300 m downstream and about 8 m off the 0° line of the incident protons. This will locate experiments in a region of acceptably low μ fluxes (Section VI).
- (2) The final beam spot size is less than 6 cm^2 .
- (3) The beam momentum is defined to better than $\pm 3\%$.

(4) Very few beam particles are lost in the magnets of the last half of the transport. This is accomplished with appropriate collimation early in the beam and is done to minimize any halo of off-energy electrons.

The beam has been designed with economic considerations in mind. Power consumption and the number of magnets and beam-tunnel enclosures have been minimized.

Since both production and multiple-scattering angles inside the Pb radiator are very small at these high energies, the electrons appear to come from the Be target with an initial source size of $0.25 \text{ cm} \times 0.25 \text{ cm}$ (see Fig. 3). This is ~ 2 times larger than the expected proton beam spot dimensions.

The transport system consists of two focusing quadrupole doublets, each convergent in both the vertical and horizontal planes. In order to have the focusing power required at energies up to 300 GeV, each doublet requires four quadrupoles. The distance from the primary target to the first doublet was chosen to obtain a large solid angle while keeping the beam spot size acceptably small in the latter part of the beam. At a downstream distance of 87 m from the target, 18 m of dipole magnets bend the electrons horizontally away from the neutral particles created in the radiator. These magnets produce a dispersion of 1.8 cm for each 1% $\Delta p/p$ at the first focus. A collimator at the first focus defines the beam momentum, and collimators at other locations in

the first leg are used to reduce beam loss in the last leg and to cut down the π/e background ratio. The aperture and location of these collimators have been determined using computer beam-transport programs and Monte Carlo techniques (see Section VI).

The quadrupole following the first focus serves as a field lens to increase the momentum acceptance. The following dipole sweeps off-momentum particles away from the beam. The second doublet system focuses the beam onto the experimental target which is 307.5 m away from the primary target. The five bending magnets following the doublet cancel the momentum-defining dispersion so that the experimental focus is achromatic. These magnets also sweep away any remaining low-energy halo.

A detailed listing of beam elements, their locations and functions, may be found in Table I. The electron transport requires nine 3 m quadrupoles, 36.5 m of dipoles, four beam enclosures, and about 550 kW at 300-GeV electron energy. The angular acceptance is about 1.2 mrad \times 2 mrad (fwhm).

IV. THE TAGGING SYSTEM

The tagging system is of a general purpose design based on previous experience at SLAC.⁴ The basic parameters of this system are listed in Table II, and a drawing of the layout is shown in Fig. 4. Referring to the figure, we shall describe the system in some detail.

The electron beam coming from the transport passes through a hole about 3.8 cm diameter in A_1 which is a multilayer lead scintillator shower veto. The electrons strike a Pb radiator with a diameter of 3.3 cm and a thickness of about 0.01 radiation lengths. The bremsstrahlung produced in the radiator passes through the magnets MT, is swept by them, and eventually reaches the experimental target (not shown). Most electrons radiate negligibly and are deflected 8.13 mrad into a dump. Those e^- which do radiate a photon between 50% and 95% of the incident energy, E_0 , are bent more strongly and will strike the sensitive region (defined by S-S) of the lead glass shower counters, T.

The energy of the e^- is then measured in two ways: by its bend in the magnet and by the pulse height produced by its shower in the Pb glass. The lead glass blocks are 7.6 cm \times 7.6 cm \times 30 cm long, each with a phototube attached. From previous experience with these blocks, we expect an energy resolution of $\pm 2\%$ at high energies. The magnetically determined momentum resolution depends on the counter location. Details of resolution, etc., may be found in Table III. Agreement between the two independent energy measurements strongly discriminates against pions and rejects other background.

In order to keep the false tag rate at an acceptably low level (10^{-3}), it is necessary to take certain precautions: low-energy electron halo and high-energy photon halo in the electron beam must be kept small; unnecessary material must be kept out of both primary

and scattered electron paths while in sight of the target (an outline of a vacuum box continuous with the beam vacuum pipe is shown); veto of background processes such as trident events in the radiator must be as complete as possible (this is the function of the anticounters A_0 , A_3 , A_4 , A_5).

V. PREDICTIONS OF e^- AND π^- YIELDS

The yield of electrons and the π/e contamination ratio as a function of energy for the beam just described have been predicted using a Monte Carlo technique. The results are shown in Fig. 5(a). As noted in Table II, one can expect 0.004 tagged photons/electron.

In generating an initial phase space for the electron beam line, the Monte Carlo program takes into account the actual physical processes that will produce e^- and π^- . Specifically included are production angular distributions in both the target and radiator, multiple scattering, attenuation and straggling.⁵ The Hagedorn-Ranft pion and nucleon yield predictions⁶ are used as calculated by Ranft's program SPUKJ.⁷ The absolute predictions should be considered only as order-of-magnitude estimates, because the Hagedorn-Ranft model has not been verified at these energies.

After the initial phase space has been generated, events are checked for acceptance at the various collimators and magnets of the beam. The transverse location of the beam particle at a given point is computed using the R matrices calculated by the program TRANSPORT.⁸

VI. ELIMINATION OF BACKGROUND CONTAMINATION

There are three basic approaches to reducing the pion component of the beam. In the primary target, neutrons are produced more sharply peaked forward than are the neutral pions that give photons. Therefore by steering the incoming protons at small angles from 0° , one can discriminate against neutrons and subsequent π^- production. At 2 mrad, for example, Monte Carlo calculations predict [Fig. 5(b)] a factor of ~ 5 reduction in π/e ratio at high energies while only reducing the e^- yield by about 3.

A second way of reducing the pion contamination depends on the difference in the angular distribution of e^- and π^- production in the radiator. The pair-production angle at energies in the hundred GeV range is $\lesssim 0.1$ mrad. Multiple scattering of the electrons in the radiator is of the same magnitude. Thus the electrons appear to come from the primary target with a spot size of the order of 0.25 cm. (The incident beam spot is expected to be half this size.) On the other hand, the π^- are produced with angles of ~ 1 mrad. Therefore, the pions appear to come from a much larger spot than the electrons as shown schematically in Fig. 3. At the images of this initial spot located at the two beam foci the pions will be spread over a larger transverse area than the electrons and thus are easily collimated. This is the function of the vertical collimator at the first focus. In practice, the magnet apertures themselves serve to limit the beam acceptance of

initial source size and thus discriminate against the pion background. The collimators are set initially so that they are at the edge of the electron distribution. If they are set tighter, the π/e ratio can be reduced further with some sacrifice of e^- intensity.

As mentioned earlier, the pion-contamination ratio can be reduced by another factor of two with a D_2 target.

Muons produced in the primary target will be swept predominately into two lobes, one charge bent up, the other down by the sweeping magnets. The beam transport bends horizontally to avoid bending into the muon flux concentration. The experimental area is located at a distance of ~325 m with a ~8 m horizontal offset in a region where muon fluxes are acceptably low.

Using a Monte Carlo program written by D. Theriot and K. Lee at NAL,⁹ we have estimated the muon fluxes at the experimental area. The program takes into account the beam shielding and the magnetic fields at the front end. We expect the muon flux to be much less than 1 muon/m^2 for 10^{13} 500-GeV protons incident. This is acceptable for all presently proposed experiments.

The most obvious way to reduce the halo of off-momentum electrons and photons to very low levels at the tagging system is to avoid beam electron losses in the last stage. These losses can be strongly controlled by blocking out particles in the first stage that would be lost in the last stage magnets. Good locations for collimators and suggestions for their apertures (Table I) were determined by studying plots

of the transverse location at elements in the first stage of particles lost in the elements of the last stage. The plots were made using the Monte Carlo program described in the last section. Trajectories calculated by TRANSPORT which are only accurate to second order were checked by tracing them through the measured fields of the beam magnets using program TURTLE written by D. Carey.¹⁰ Both calculations indicate last leg losses of $\sim 10^{-3}$ of the beam intensity with the collimation noted in Table I. Most of these losses come at the first quadrupole of the second stage doublet.

Losses in the beam pipe can be reduced by making the diameter of the pipe large. (Because of multiple scattering and radiative losses, the whole length of the beam pipe must be under vacuum.) If the beam pipe is 20 cm in diameter, the minimum grazing and rescattering angle of particles that are accepted by the magnet apertures is ~ 2 mrad. There are negligible numbers of secondary electrons of energy above 15 GeV produced at angles greater than 2 mrad.⁵

The question remains of what kind of halo will be caused by the small losses ($\sim 10^{-3}$ e⁻ intensity) in the last stage magnets. This problem has been treated both by hand⁵ and using a Berkeley program LASER.^{5,11} Both calculations agree that the off-momentum halo will be safely less than 10^{-6} of the beam intensity. This is an order of magnitude better than the most stringent experimental requirement.

The Monte Carlo program LASER indicates that the probability that a shower electron originating within 0.001 cm of the edge of one of the last quadrupoles reaches the tagging target within 7.5 cm of the beam line is less than 0.02 with 90% confidence. The probability decreases sharply at greater depths. (At very shallow depths, the probability is larger, 0.07, if the shower originates in the first 10^{-5} cm. There are no important cascade effects, however, because even inside the iron the probable maximum number of shower electrons with energy above 15 GeV going to one side is never above 0.85 per initial electron.¹²⁾ With a magnet aperture of ~7.5 cm, the fraction of electrons per cm is $1/7.5 \text{ cm}^{-1}$, assuming a flat distribution. In fact, the Monte Carlo plots indicate that at the magnet walls the intensity has fallen by $\gg 10$. Therefore assuming a beam density of $1/75 \text{ cm}^{-1}$ at the edges is an overestimate. This corresponds to 1.3×10^{-5} electrons within 0.001 cm of the edge per beam electron. Multiplying by 0.02, this gives a probability of a shower electron reaching the tagging system of less than 3×10^{-7} per beam particle.

VII. FUTURE IMPROVEMENTS OF THE FACILITY

The facility described here was designed for low cost, reliability, and ease of installation. Future experimenters may desire improvements in the momentum resolution and/or the π/e ratio. Both may be accomplished by extending the beam another two stages.⁵

With a nondispersed focus available for collimation, the pion contamination can be reduced by a significant factor. This will require use of sextupoles to eliminate second-order smearing of the image. The π/e contamination ratio may be reduced by one to two orders of magnitude by installing a very high magnetic field between two separate momentum-defining segments of the beam. At high energies and fields of 50-100 kG over a few meters, the electrons will lose up to 5% of their energy to synchrotron radiation. Since the pions will be essentially unaffected, a very strong discrimination against pions is possible by tuning the subsequent sections of the beam to the shifted electron momentum. The high magnetic field may be inserted in the beam in one of two ways: by replacing a conventional bending magnet string with a pair of very high field magnets with field of opposite sign so that the original bending angle is reproduced,⁵ or by use of a three magnet "chicane" system (fields $+-+$) which does not affect the ultimate path of the beam.¹³

If hodoscopes are installed to measure beam electron transverse positions, it is possible to improve the momentum resolution of the electron beam to the $\pm 0.2\%$ level without reducing the acceptance of the beam. This is most safely done in the latter stages of a long beam where the muon fluxes are low. Hodoscopes can also be used to define with precision the angle of beam particles at the experimental target. If desired, the resolution of the tagging system can be improved to

~0.5%. Space has been included for possible future use of proportional wire chambers to define the scattered electron trajectory more accurately.⁵

VIII. ACKNOWLEDGMENTS

All of us would like to acknowledge the hospitality of NAL while we worked on this design.

We have had useful discussions and help from the following:

C. Heusch, G. Knies, J. J. Murray, A. L. Read, D. Reeder, A. Seiden, S. C. C. Ting, and J. Walters. We particularly appreciated the support and help from A. L. Read who acted as moderator during our group's working meetings at NAL.

Table 1. Electron Transport Beam Elements.

| Position ^a (m) | Name | Size (Magnet Type ^b) | Field Strength kG at Pole Tip | Function |
|------------------------------|------------------------------|-------------------------------------|----------------------------------|--|
| 0 | Be target | 36 cm thick | ———— | Produce γ 's |
| 7.6 | Sweeping magnets | 5-1.5-600 | 15 | Sweep charged particles away from radiator |
| 22.0 | Pb radiator | 0.5 rad. lengths | ———— | Convert γ to e^+e^- |
| 30.8 | Q ₁ | 3Q-120 | 5.79 | First quad doublet: create first focus |
| 34.1 | Q ₂ | 3Q-120 | 5.79 | |
| 39.0 | Q ₃ | 3Q-120 | -4.92 | |
| 42.3 | Q ₄ | 3Q-120 | -4.92 | |
| 43.9 | Collimator 1 | 6.0 cm vert. | ———— | Reduce 2nd leg losses |
| 77.7 | Collimator 2 | 3.4 cm horiz. | ———— | Reduce 2nd leg losses and define beam size |
| 80.8 | M1 | 2-1.5-240 | 14 | Produce dispersion and bend away from 0° line |
| 87.2 | M2 | 2-1.5-240 | 14 | |
| 93.6 | M3 | 2-1.5-240 | 14 | |
| 158.8 | Collimator 3 F1 | 7.6 cm horiz. 0.6 cm vert. | ———— | First focus. Momentum definition to $\pm 2\%$. Define nonbend plane source size to reduce π/e |
| 160.6 | Q5 | 3Q-120 | 3.43 | Field lens, reduces dispersion, so increases P acceptance |
| 163.6 | M4 | 5-1.5-120 | 12 | Sweep off-momentum particles and cancel dispersion |
| 231.6 | Q6 | 3Q-120 | -4.50 | Second quad doublet. Focus on experimental target (F2) |
| 235.0 | Q7 | 3Q-120 | -4.50 | |
| 239.8 | Q8 | 3Q-120 | 4.57 | |
| 243.2 | Q9 | 3Q-120 | 4.57 | |
| 246.5 | M5 | 5-1.5-120 | 11.9 | Sweep low energy particles; cancel dispersion and make beam achromatic at F2 |
| 249.9 | M6 | 5-1.5-120 | 11.9 | |
| 253.2 | M7 | 5-1.5-120 | 11.9 | |
| 256.6 | M8 | 5-1.5-120 | 11.9 | |
| 259.9 | M9 | 5-1.5-120 | 11.9 | |
| 266.3 | Pb tagging target | 0.01 rad. lengths | ———— | Produce bremsstrahlung |
| ~ 271 | Tagging magnets and counters | | | Momentum analyze scattered e^- , define γ momentum, sweep beam |
| 307.5 | Experimental target | | | |

^aPosition at center of element.^bMagnet Type Code: Dipoles - width, height, length (in.)
Quadrupoles - diameter, - Q - length (in.)

Table II. Photon Tagging System Parameters.

| | |
|--|---------------------------------|
| Incident electron energy range, E_0 | 22 to 300 GeV |
| Tagged photon energy range | ($\leq 65\%$ to 95%) E_0 |
| Tagged photons <u>per</u> incident electron (1% radiator) | 4×10^{-3} |
| Contribution to photon energy uncertainty from tagging system | $\leq \pm 2\%$ |
| False tag rate | $< 0.1\%$ |
| Bend for nonradiating electrons | 8.13 mrad |
| Number of magnets | 4 |
| MT_0 | 0.1 kG · m |
| MT_1 | 34.9 kG · m |
| MT_2 | 23.4 kG · m |
| MT_3 | 22.9 kG · m |
| $\int Bdl$ at 300 GeV | 81.3 kG · m |
| Magnet power at 300 GeV | 115 kW |
| Counters | |
| Scintillation | 10 |
| Lead-Scintillator | 1 |
| Lead-glass | 11 |
| Space required | |
| Length | 20 m |
| Clearance from beam on all sides | 0.8 m |

Table III. Tagging System Resolution.

| Tagging Counter | T ₁ | T ₂ | T ₃ | T ₄ | T ₅ | T ₆ | T ₇ | T ₈ | T ₉ | T ₁₀ | T ₁₁ | |
|---|----------------|----------------|----------------|----------------|----------------|----------------|----------------|----------------|----------------|-----------------|-----------------|-----|
| Mean recoil electron energy | 14 | 18 | 25 | 38 | 45 | 55 | 62 | 70 | 85 | 115 | 150 | GeV |
| Recoil electron energy resolution | ±4.3 | 3.8 | 3.2 | 2.6 | 2.3 | 2.2 | 2 | 2 | 2 | 2 | 2 | % |
| | ±0.6 | 0.7 | 0.8 | 1.0 | 1.0 | 1.2 | 1.2 | 1.4 | 1.7 | 2.3 | 3.0 | GeV |
| Mean tagged photon energy | 286 | 282 | 275 | 262 | 255 | 245 | 238 | 230 | 215 | 185 | 150 | GeV |
| Tagging contribution to photon energy uncertainty | ±0.2 | 0.3 | 0.3 | 0.4 | 0.4 | 0.5 | 0.5 | 0.6 | 0.8 | 1.3 | 2.0 | % |
| Worst case geometrical resolution | ±1.5 | 2.1 | 3.3 | 1.9 | 2.4 | 2.9 | 3.4 | 4.3 | 8.4 | 16 | >±50 | % |

REFERENCES

¹The concept of an electron-photon beam at a high-energy proton synchrotron was suggested in early NAL design studies. The following list is not exhaustive:

- C. A. Heusch, 200-BeV Accelerator, 1966 Summer Study, Lawrence Radiation Laboratory Report UCRL-16830, Vol. III, p. 156.
- W. T. Toner, 1968 NAL Summer Study, Vol. 2, p. 125.
- C. A. Heusch, 1968 NAL Summer Study, Vol. 1, p. 153.
- R. Diebold and L. Hand, 1969 NAL Summer Study, Vol. 1, p. 153.
- C. A. Heusch, 1969 NAL Summer Study, Vol. 1, p. 163.
- R. Morrison, K. Pretzl, and A. L. Read, 1970 NAL Summer Study, p. 39.
- A. Mischke et al., 1970 NAL Summer Study, p. 369.
- R. Morrison et al., Proc. International Conference on Instrumentation for High Energy Physics, Dubna, 1970, p. 734.

A beam following the same general concept as this one has been constructed at Serpukhov. A report was made to the International Conference on Instrumentation for High Energy Physics, Dubna, 1970, by A. L. Alikhanian et al. "Preliminary Data on Electron Beams at Momenta Larger than 30 BeV/c at the Serpukhov Proton Synchrotron," IHEP 70-105.

²The probability of pair production per unit radiation length for a very high energy photon is $\sim 7/9 \approx 0.77$. [B. Rossi, High-Energy Particles, Eq. 2.19 (13).]

³Review of Particle Properties, Particle Data Group, Rev. Mod. Phys. 43, S1 (1971).

⁴D. O. Caldwell, V. B. Elings, W. P. Hesse, G. E. Jahn, R. J. Morrison, F. V. Murphy, D. E. Yount, Phys. Rev. Letters 23, 1256 (1969).

⁵Further details concerning these calculations may be found in the appendix of the "Report of the Working Group on a Tagged Photon-

Electron Beam Facility for NAL, " National Accelerator Laboratory
Report FN-240, 1972.

⁶R. Hagedorn and J. Ranft, Suppl. Nuovo Cimento I 6, 169 (1968).

⁷J. Ranft, The Computer Program SPUKJ, Karl-Marx U., TUL-37,
July 1970.

⁸Karl L. Brown and Sam K. Howry, Transport/360, SLAC Report
91, July 1970.

⁹D. Theriot and K. Lee (National Accelerator Laboratory), personal
communication, 1972.

¹⁰D. Carey (National Accelerator Laboratory), personal communication,
1972.

¹¹LASER, written by William Podolsky and M. Rabin, personal com-
munication.

¹²B. Rossi, ibid, Eq. 5.13, p. 248.

¹³F. J. M. Farley, E. Picasso, and L. Bracci, CERN NP Internal
Report 71-11.

FIGURE CAPTIONS

Fig. 1. Schematic view of tagged photon-electron facility for NAL.

Fig. 2. Monte Carlo predictions of electron yields and π/e ratio vs radiator thickness at $E_e = 100$ GeV. (10^{13} 500-GeV protons on 36-cm Be assumed.)

Fig. 3. Schematic drawing of production angles of e^- and π^- in radiator showing effective image size seen by transport.

Fig. 4. Photon tagging system. 300-GeV electrons are shown incident from the left. MT_0 through MT_3 are magnets with fields into the paper which bend a total of 8.13 mrad. A_1 through A_5 are scintillation veto counters. S-S are scintillation counters to define the active area of T_1 through T_{11} , the lead-glass tagging counters. The electron beam dump would be at 22 m.

Fig. 5. Monte Carlo prediction of electron yield and π/e ratio vs energy with 0.5 r.l. Pb radiator. (10^{13} 500-GeV protons on 36 cm Be assumed.)

a) 0 mrad proton incident deflection.

b) 2 mrad horizontal proton deflection.

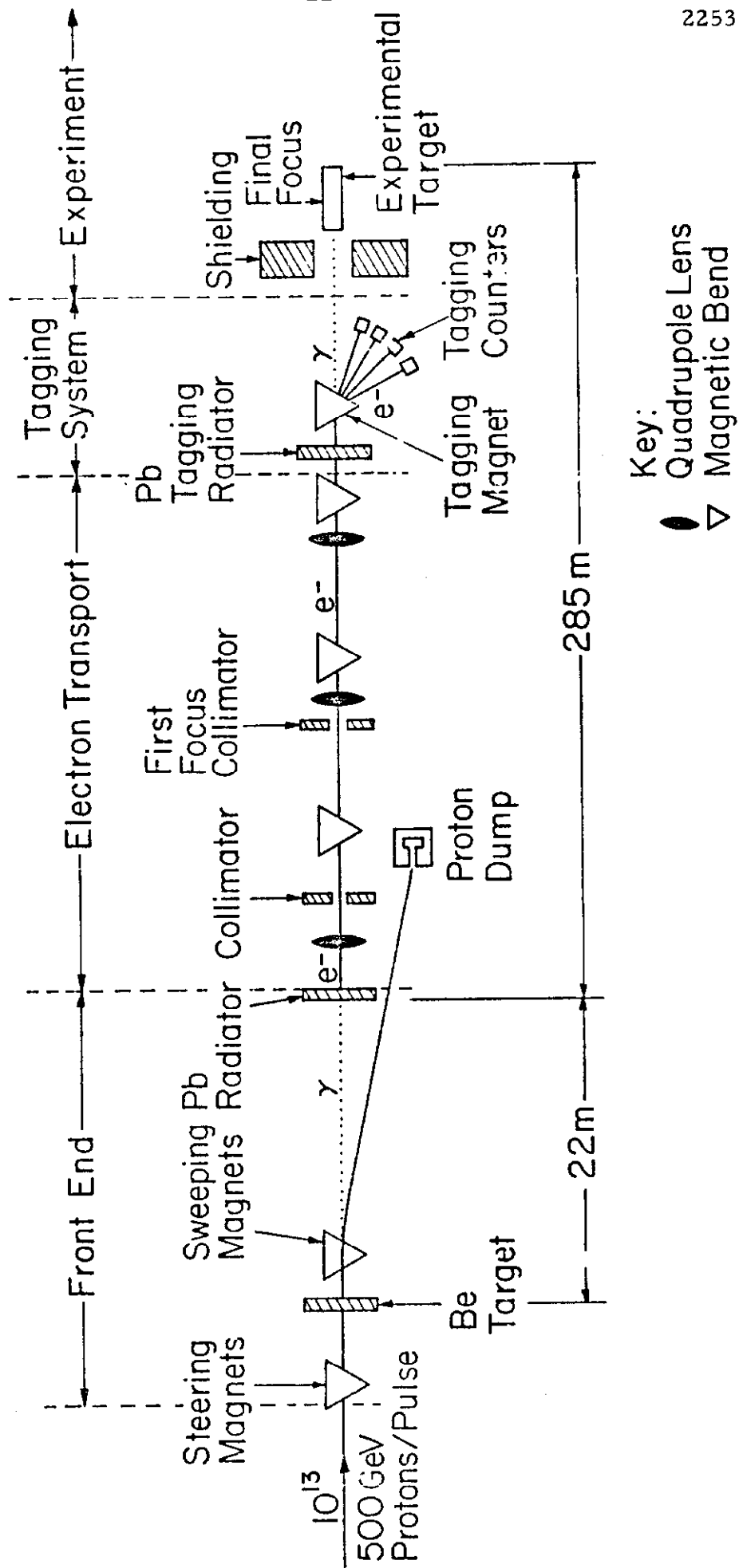


Fig. 1

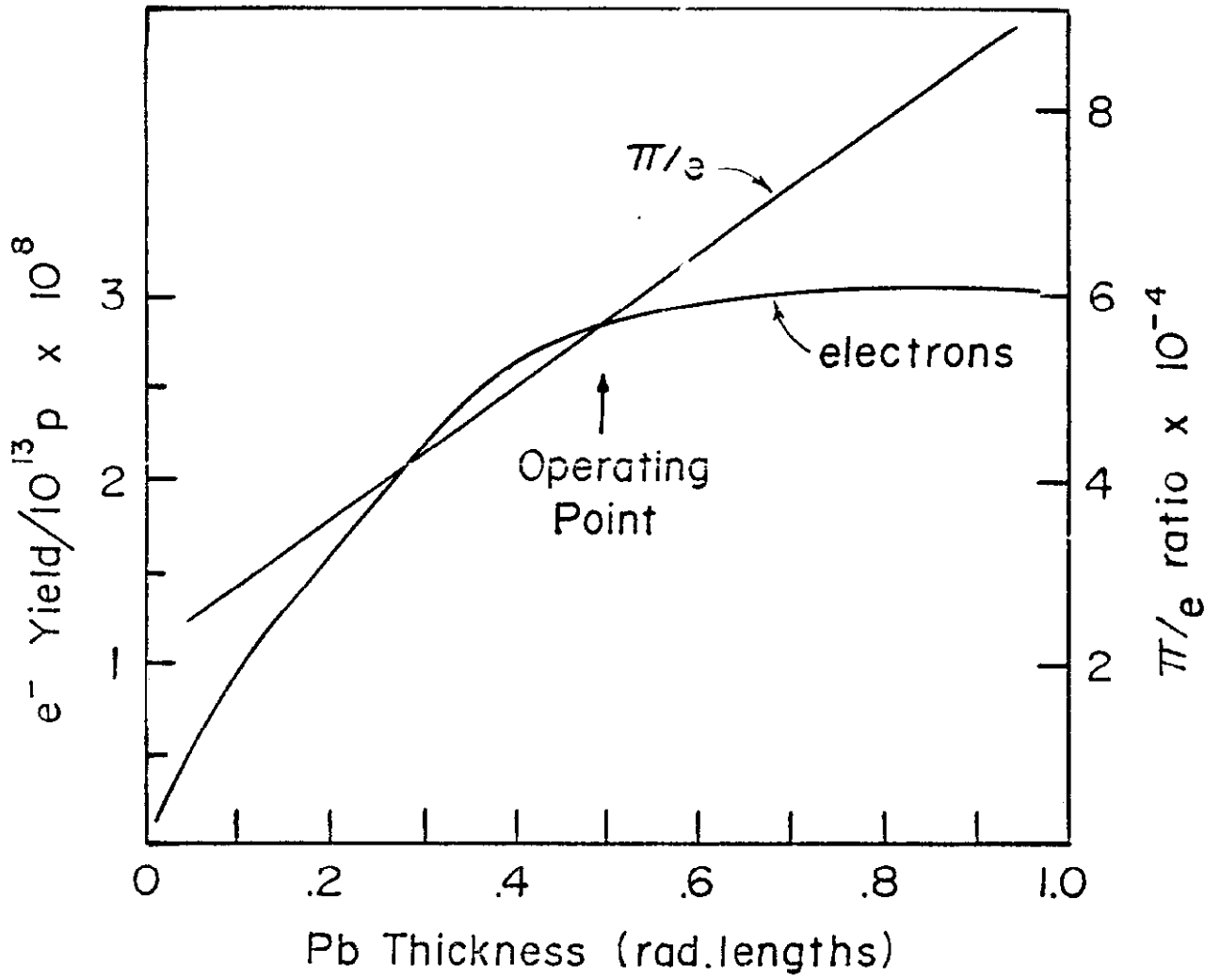


Fig. 2

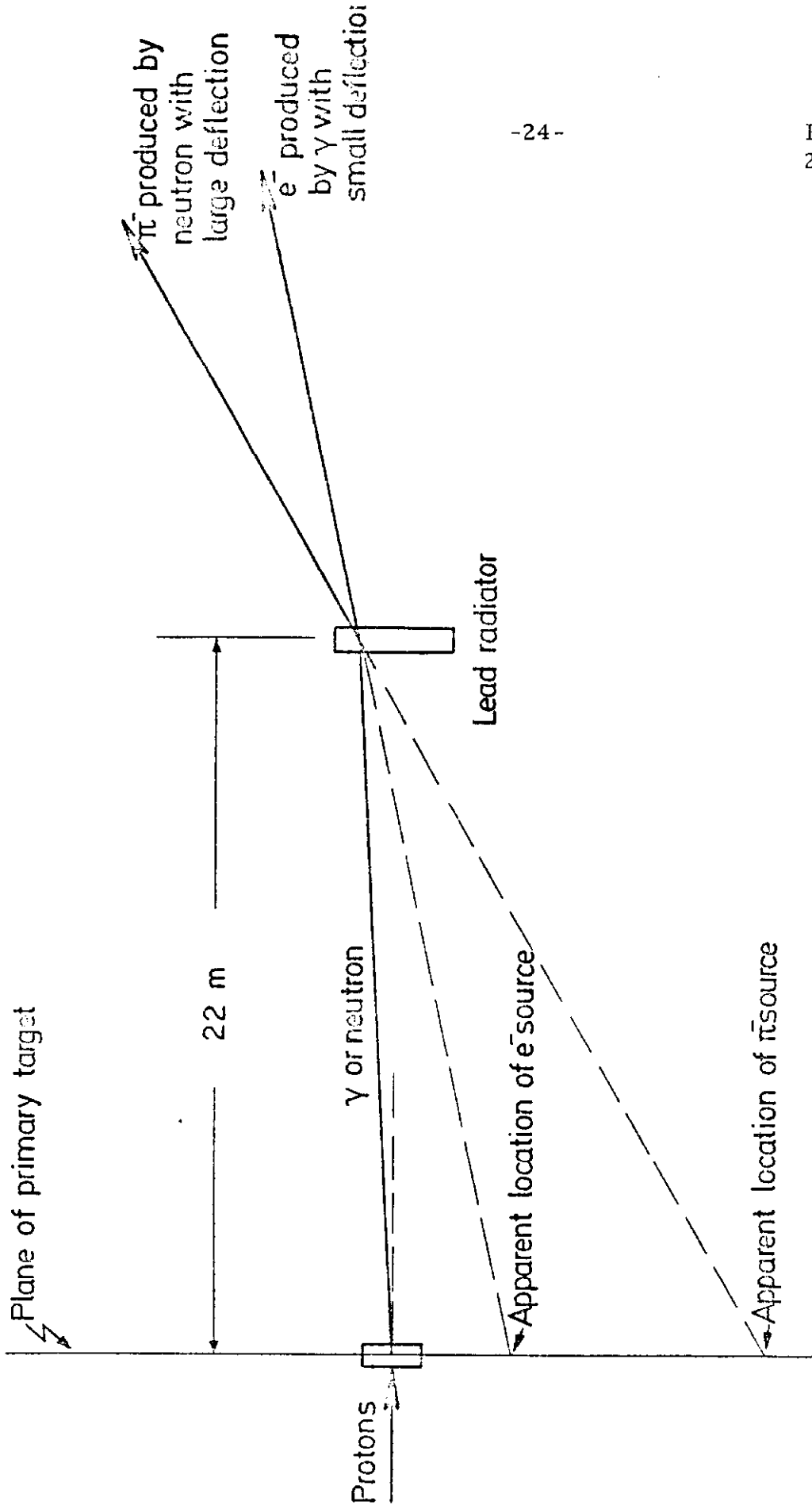


Fig. 3

SIDE VIEW

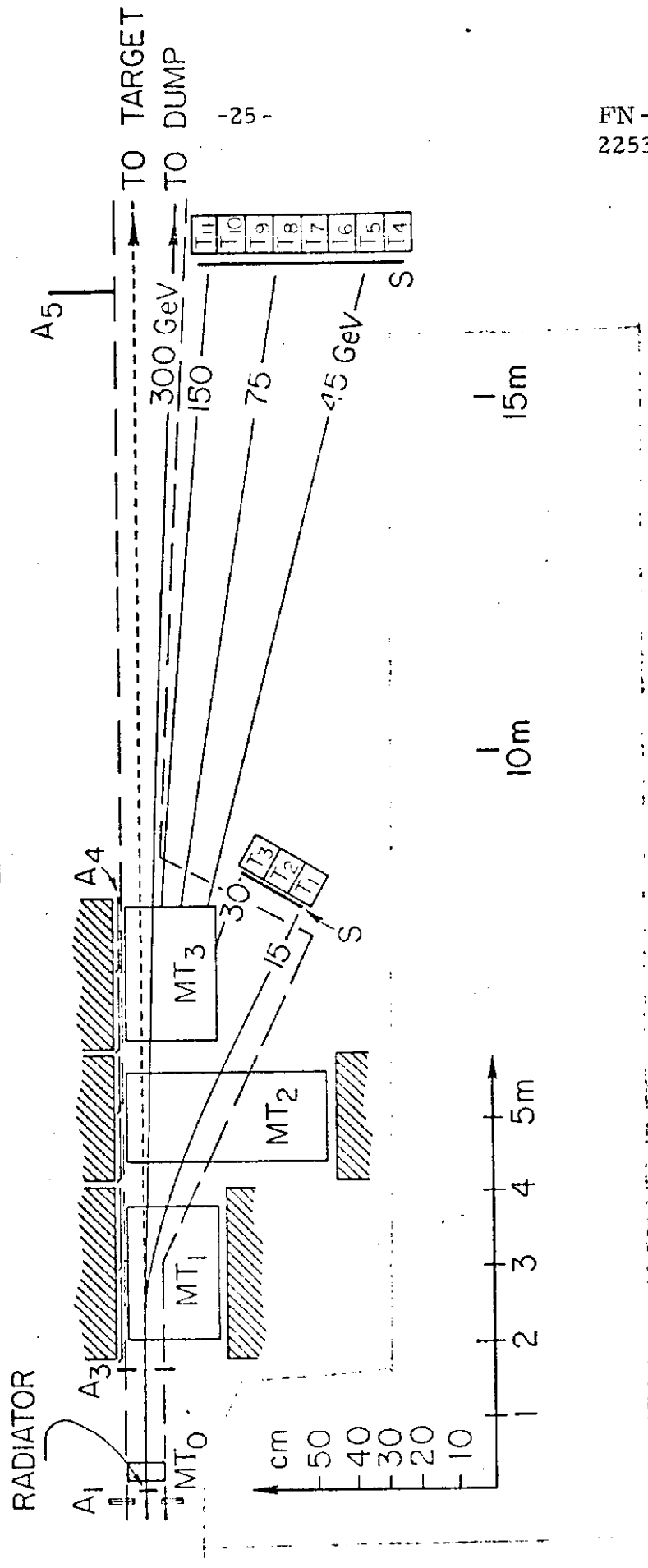


Fig. 4

FN-241
2253.000

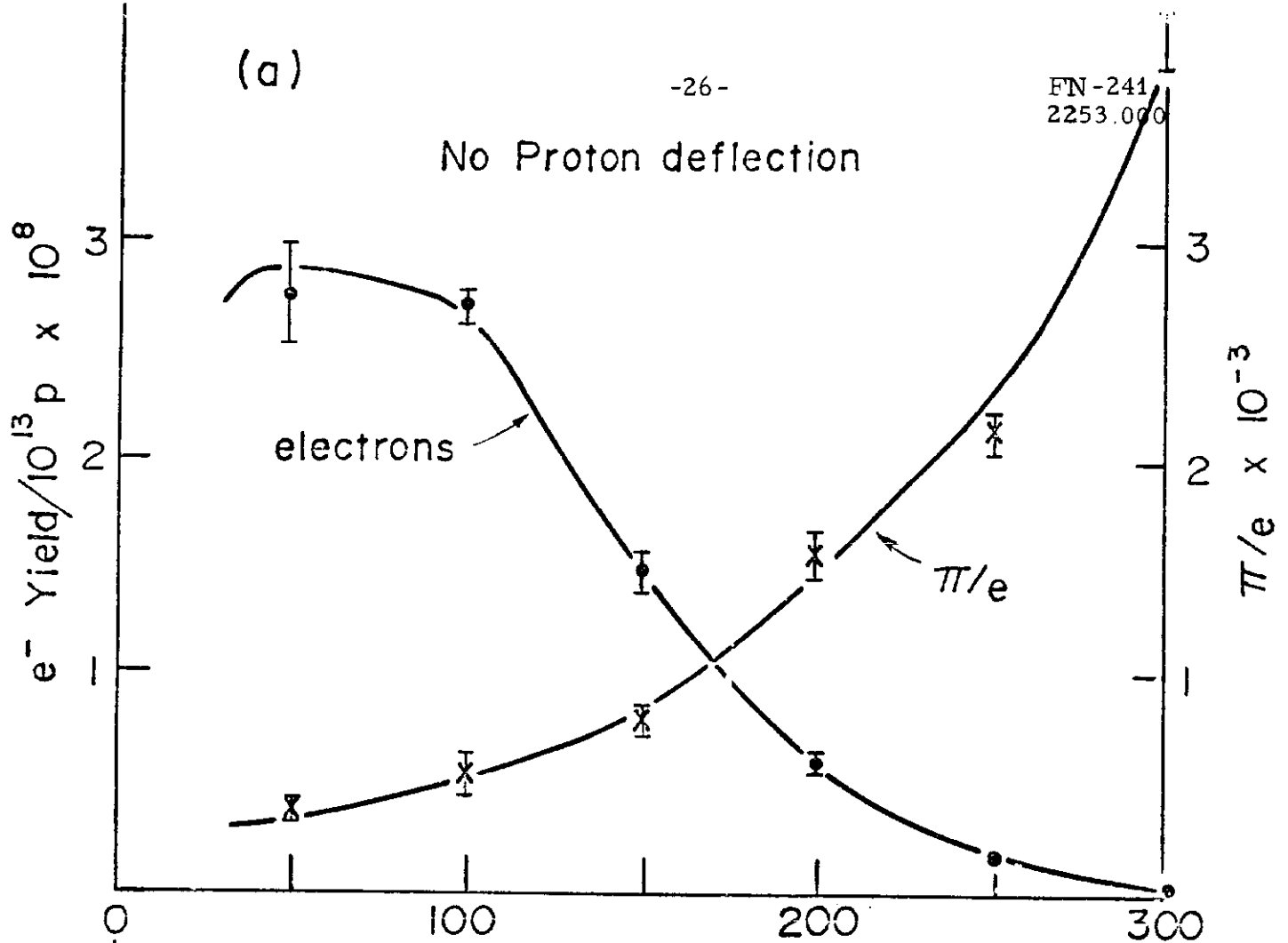


Fig. 5

